ELSEVIER

Journal of Organometallic Chemistry 564 (1998) 167–177

Journal of Organometallic Chemistry

Base-free tris(indenyl)lanthanoid(III) complexes (Ln = La, Pr, Nd, Sm): solid-state structure and solution NMR/NIR–vis spectroscopy

Jingwen Guan, R. Dieter Fischer *

Institut für Anorganische und Angewandte Chemie, Universität Hamburg, Martin-Luther-King-Platz 6, D-20146 Hamburg, Germany

Received 23 February 1998; received in revised form 27 April 1998

Abstract

Strictly base-free, well-crystallized $[M(C_9H_7)_3]$ (C_9H_7 = indenyl) with M = Nd **3**, Pr **4** and La **5** was probably prepared for the first time from the corresponding tetrahydrofuran adducts, $[M(C_9H_7)_3 \cdot THF]$. According to X-ray crystallographic studies, the crystal parameters and molecular conformations of **3**, **4** and **5** differ from those already reported for the homologues with M = Sm **1** and U **2**. While the conformation of the isostructural complexes **3** and **4** remains, nevertheless, reminiscent of that of **2**, the molecular architecture of **5** is, at least at lower temperature, notably different and more similar to that of some earlier reported Lewis base (L) adducts, $[Ln(C_9H_7)_3 \cdot L]$. Actually, **5** consists of infinite, polymeric zigzag chains, $[La(\eta^5\text{-}C_9H_7)_2(\mu\text{-}\eta^1{:}\eta^5\text{-}C_9H_7)]_\infty$, owing to one relatively short intermolecular La…C′ contact of 309.7(4) pm. While crystalline **4** involves isolated molecules, variable-temperature ^{1}H-NMR spectra suggest that, inter alia, in $C_6D_5CD_3$ and CD_2Cl_2 solution short-lived oligomeric species compete increasingly in concentration with the monomer as the temperature is lowered.

Keywords: Lanthanoid; Conformation; Indenyl; Crystal structure

1. Introduction

Since about 1990, numerous new details on the structural chemistry of 1:1 base adducts of the complex type $[Ln(III)(C_9H_7)_3 \cdot L]$ (Ln = lanthanoid element; C_9H_7 = indenyl anion; L = uncharged Lewis base) have been contributed by several research groups [1–7]. According to these results, the conformational diversity of crystalline $[Ln(III)(C_9H_7)_3 \cdot L]$ systems is notably richer than it had earlier been anticipated. In contrast, the crystal structures of no more than two base-free, homoleptic $[M(C_9H_7)_3]$ species are known (**1**, M = Sm [8], **2**, M = U [9]). The conformation of **2** resembles those of its halogenated derivatives $[U^{IV}(C_9H_7)_3X]$ with X = Cl [10] and Br [11], where the benzo groups of the three indenyl ligands are oriented *meridional* in an all-*cisoid* fashion (i.e. towards the axial ligand X). The three likewise *meridional* benzo groups of **1** are, on the other hand, no longer all-*cisoid*. While the structure of **2** corresponds to the earlier-defined type D [5], that of **1** is so far unprecedented.

Interestingly, the ionic radius of U(III) approaches closely that of La(III) [12]. As the crystal structures of both **1** [8] and **2** [9] are devoid of any intermolecular contacts, the tendency of their homologues with Ln = Nd **3**, Pr **4** and La **5** to undergo self-association in the crystal is expected to be likewise quite low. Intermolecular contacts are, however, quite important for the structures of the base-free $[Ln(C_5H_5)_3]$ and $[Ln(C_5H_4Me)_3]$ complexes of the early Ln elements [13]. In the following, the crystal and molecular structures of **3**, **4** and **5** are reported along with some relevant spectroscopic properties of these complexes in solution.

* Corresponding author. Fax: +49 404 1232893.

0022-328X/98/$19.00
PII S0022-328X(98)00637-8

Table 1
Survey of crystal data and details of data collection and refinement for **3–5**

	3	**4**	**5**
Empirical formula	$C_{27}H_{21}Nd$	$C_{27}H_{21}Pr$	$C_{27}H_{21}La$
Formula weight	489.68	486.35	484.35
Temperature (K)	293(2)	293(2)	153 (2)
Diffractometer	Syntex $P2_1$	Syntex $P2_1$	Hilger and Watts Y290
Wavelength (pm)	71.073	71.073	71.073
Crystal system	Orthorhombic	Orthorhombic	Monoclinic
Space group	$P2_12_12_1$	$P2_12_12_1$	$P2_1$/c
Unit cell dimensions			
a (pm)	994.1(5)	993.9(4)	1400.2(7)
b (pm)	996.3(5)	997.9(6)	1346.0(7)
c (pm)	2054.9(10)	2064.9(9)	1022.4(5)
β (°)	—	—	92.02(2)
Volume (nm^3)	2.035(2)	2.048(2)	1.926(2)
Z	4	4	4
$D_{calc.}$ (g cm^{-3})	1.598	1.577	1.671
μ (mm^{-1})	2.560	2.387	2.227
$F(000)$	972	968	960
2θ range for data collection (°)	4.5–50	4.5–50	5–55
Index ranges			
h (°)	−4 to 11	−1 to 11	−18 to 18
k (°)	−2 to 11	−2 to 11	−17 to 4
l (°)	−9 to 24	−1 to 24	−2 to 13
Reflections collected	3591	2832	6578
Independent reflections (R_{int})	2917 (0.0473)	2560 (0.0411)	4273 (0.0576)
Data/restraints/parameters	2916/0/253	2560/0 /253	4271/0/254
Goodness of fit on F^2	1.093	1.131	1.073
Final R indices [$I>2\sigma(I)$] R_1/wR_2	0.0460/0.1112	0.0530/0.1177	0.0385/0.0949
R indices (all data) R_1/wR_2	0.0531/0.1183	0.0712/0.1300	0.0454/0.1010
Absolute structure parameter	−0.02(5)	−0.01(5)	—
Largest difference peak and hole (e nm^{-3})	845 and −1370	1297 and −720	1928 and −1441

2. Preparation and general properties of 1 and 3–5

Although the facile preparation of base-free $[Ln(C_9H_7)_3]$ systems from the corresponding THF-adducts is suggested in the early literature [14], we have found only recently [7] that complete

$$[(C_9H_7)_3Ln\cdot THF] \overset{\text{vacuum, }\Delta}{\rightarrow} [Ln(C_9H_7)_3] + THF \qquad (1)$$

THF-removal requires more efforts than initially reported. According to our experience, strictly THF-free complexes are obtained best when the thermal degradation is carried out at (a) higher temperatures (i.e. between 120 and 150°C), (b) a better vacuum (i.e. $\leq 1 \times 10^{-3}$ mbar) and (c) when this process is extended over sufficiently long periods (for at least 5 h). Otherwise, significant amounts of THF will still remain in the sample, and can readily be detected by means of X-ray diffractometry, NMR spectroscopy, elemental analysis, etc. [7]. The base-free complexes **1** and **3–5** are, as their base adducts, extremely sensitive to air and moisture. In THF and CH_2Cl_2 the solubility of **1** and **3–5** is comparable with that of their THF-adducts, while both in benzene and toluene the solubility of the base-free complexes exceeds that of their adducts. All complexes are stable towards CH_2Cl_2 for several hours. Although **1** and **3–5** are thermally stable up to at least 180°C, their tendency to sublime under the above conditions is surprisingly poor. In the mass spectra the metal-containing main fragments $[Ln(C_9H_7)_n]^+$ with $n = 1–3$ are readily detectable.

Interestingly, the base-free $[Ln(C_9H_7)_3]$ systems differ notably in colour from their THF-adducts, which feature seems to be more pronounced than for corresponding pairs of base-free and base-containing tris(cyclopentadienyl) complexes [7] (exceptions are, however, the cerium(III) complexes, $[Ce(C_5H_4R)_3]$, which are blue without, and yellow with, an additional ligand L—see ref. [13]). Thus **1** is greyish–red (the adduct is deep red), **3** violet–red (the adduct is green), **4** deep red (the adduct is pale green), and **5** faintly yellow (the adduct is almost colourless). For the dissolved complexes, the colours remain essentially the same as in the solid state (vide infra).

3. Crystallographic results for 3–5

Single crystals of **3**, **4** and **5** suitable for X-ray crystallographic studies were grown from concentrated toluene solutions. Table 1 presents the crystal data of

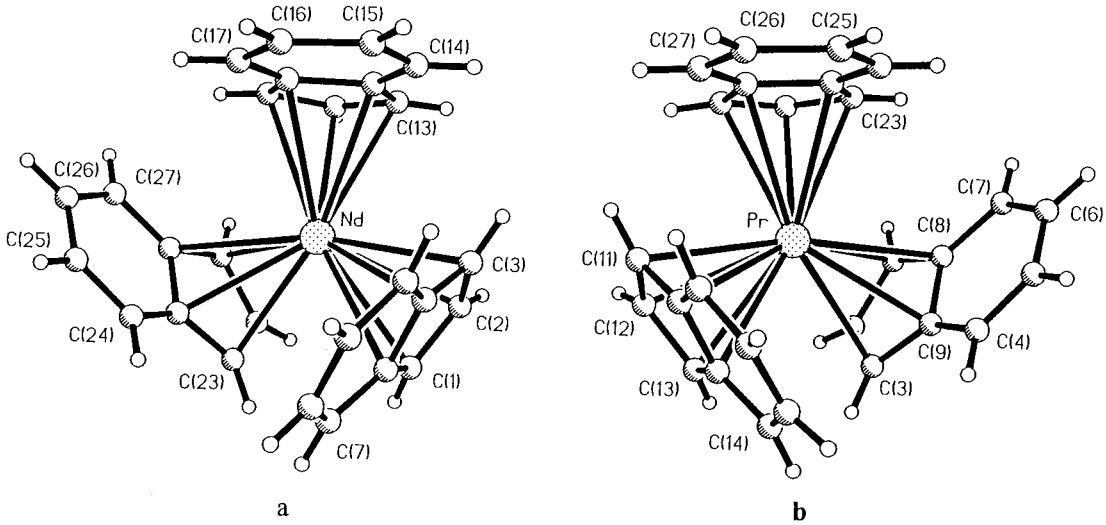

Fig. 1. Structural perspectives and atomic numbering schemes of complexes **3** (a) and **4** (b). Note that the two molecules may be considered as non-superimposable mirror images.

the three complexes details and of data collection and refinement. Perspectives of the molecular structures of **3** and **4** are given in Fig. 1, while the molecular structure for **5** is illustrated in Fig. 2. While **3** and **4** are isostructural, although the resulting molecules turn out to be mutual mirror images, molecule **5** adopts a strongly different structural pattern. The conformations of **3**, **4** and **5** differ, moreover, from those reported for **1** [8] and **2** [9]. Fig. 3 presents schematic views of the structures of **3**, **4** and **5**, wherein the positions of the metal ion and the centers of the six-membered (benzo-) rings, respectively, are referred to the plane spanned by the centers of the three five-membered (cyclopentadienyl) ring fragments of the indenyl ligands. The corresponding distances of Ln atoms and the ring centers Ct from that plane are collected in Table 2. These data quantify the actual extent to which each individual 'indenyl vector' deviates from the ideal *equatorial* or *meridional* orientation.

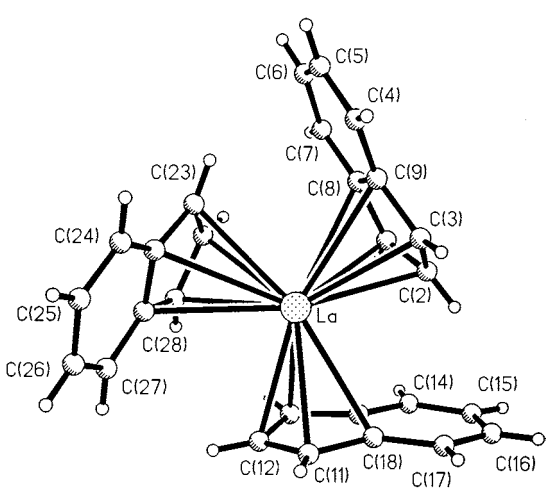

Fig. 2. Structural perspective and atomic numbering scheme of **5**.

Admittedly, **1**–**4** have in common that all three benzo groups are disposed either ideally, or at least approximately, *meridional*, which orientation appears to be particularly attractive for base-free systems [5–7]. In contrast, each molecule of **5** involves two *equatorially* head-to-tail oriented indenyl ligands, and consequently also *chirogenic* $\{La(C_9H_7)_3\}$ units [5]. The conformational pattern of **5** resembles those realized in several Lewis base adducts, $[Ln(C_9H_7)_3 \cdot L]$ [5,7]. While, in accordance with the achiral space group $P2_1/c$, both enantiomers of **5** are present in equal amounts, **3** and **4** actually crystallize in the chiral space group $P2_12_12_1$. One possible origin of this chirality could be the asymmetrical orientation of one only quasi-*meridional* C_9H_7 ligand, the presence of which actually deprives the molecule of any non-trivial symmetry element. In fact, the two perspectives of **3** and **4**, shown in Fig. 1, resemble non-superimposable mirror images, suggesting that the two selected single crystals of **3** and **4** had accidentally involved the corresponding quasi-enantiomers.

Selected bond distances and angles of **3**–**5** are collected in Table 3. The individual Ln–C distances involving indenyl carbon atoms in the positions 1, 2 and 3 (following here the conventional nomenclature rules) of **3**–**5** compare well with the corresponding Ln–C bond distances of 1:1 base adducts of the same Ln element. On the other hand, the Ln–C distances involving the indenyl carbon atoms 8 and 9 (belonging to both the five- and the six-membered ring) seem to depend frequently on the actual orientation of the benzo group. While in **5** wherein two C_9H_7 ligands are *equatorial* the La–C(8/9) distances exceed the La–C(1/2/3) contacts significantly, these two categories of Ln–C distances differ notably less for **3** and **4** which

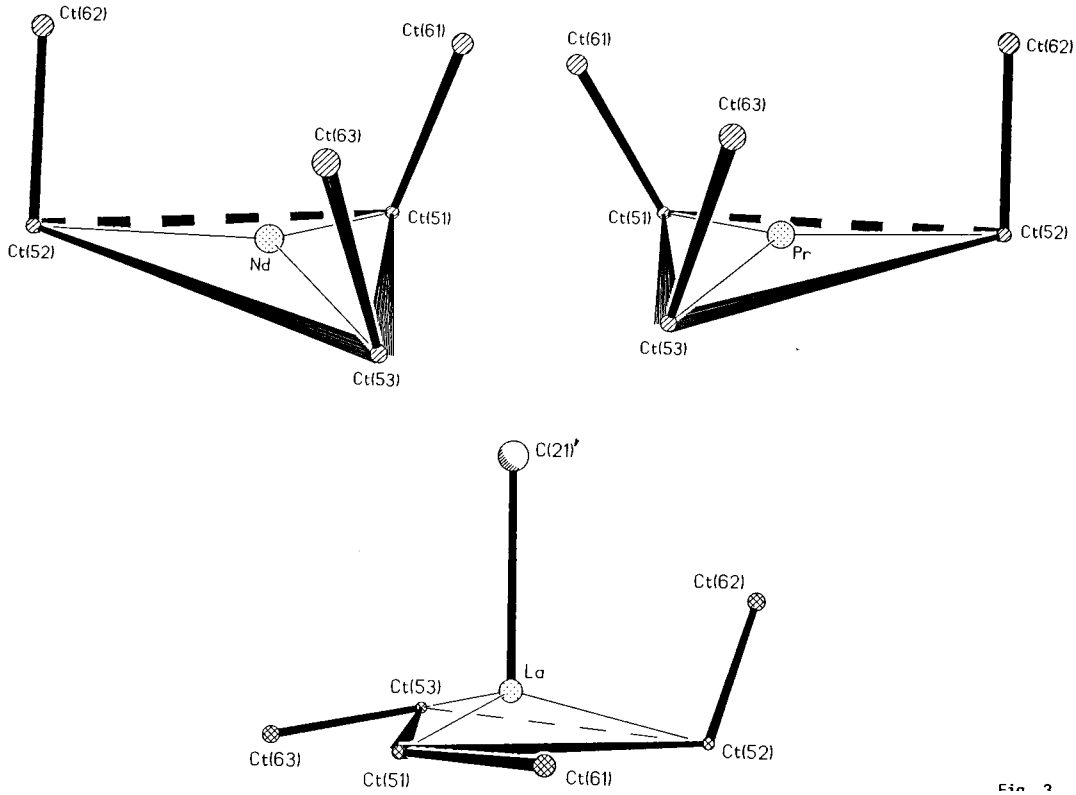

Fig. 3. Simplified perspective of the structures of **3** and **4** (top) and **5** (bottom) based on the positions of the central metal ions and of the C_5- and C_6-ring centers of the indenyl ligands only (the atom C(21)′ belongs to an adjacent molecule).

complexes involve three (quasi-)*meridional* C_9H_7 ligands (see Table 4). Likewise, for the complexes **1** and **2** wherein all three C_9H_7 ligands are (quasi-)*meridional*, again almost equal Ln–C(1,2,3) and Ln–C(8,9) contacts have been reported [8,9]. In Table 4, the quantity $\Delta = \langle \text{Ln–C}(8, 9)\rangle_{av} - \langle \text{Ln–C}(1, 2, 3)\rangle_{av}$ is compared for a number of crystallographically-investigated tris(indenyl)lanthanoid complexes. Deviations from the *meridional* C_9H_7 disposal usually cause a widening of the Ln–C(8,9) contacts and lead to Δ values >10 pm. Concomitantly, non-*meridional* C_9H_7 ligands turn out to be more strongly folded about their C8–C9 axis than *meridional* C_9H_7 ligands. Thus the corresponding dihedral angle ϕ of **3** and **4** is particularly small. Actually, increasing non-coplanarity of the C_5- and C_6 portions of the indenyl unit reflects, like increasing Ln–C(8,9) contacts, substantial steric congestion. The data of Table 4 also demonstrate that the steric congestion in total increases as the ionic radius of the metal ion decreases.

Table 2
Survey of the distances of the metal ion and the various C_6-ring-centers, Ct(6n), respectively, from the planes spanned by the corresponding five-ring-centers Ct(5n) (distances in pm)

Sample/Ln	Metal Ion	Ct(61)	Ct(62)	Ct(63)
3 Nd	20.8	211.4	195.4	194.8
4 Pr	21.1	197.7	210.5	195.0
5 La	54.6	14.7	−38.4	182.8

4. The polymeric nature of complex 5

A closer inspection of the molecular packing in the crystals of **3**, **4** and **5** confirms that **3** and **4** should be considered as isolated molecular units, while the lattice of **5** turns out to consist of infinite, polymeric zigzag chains (see Fig. 4). One 1- or 3-positioned ring carbon atom of the non-*equatorial* C_9H_7 ligand of each $[La(C_9H_7)_3]$ molecule is found to contact the La center of an adjacent molecule (Fig. 4) in that an intermolecular La…C distance of 309.7(4) pm results. The next-shortest intermolecular La…C distance amounts to 329.4 pm. The 309 pm contact compares favourably with corresponding intermolecular Ln…C distances reported for various poly- or oligomeric cyclopentadienyl complexes of La(III) and related metal ions of almost identical size (Table 5). Except for one of the two different $[La(C_5H_5)_3]_\infty$ modifications and the dinuclear adduct involving Sm(II) and Sm(III), all examples compared in Table 5 are based on one singular intermolecular Ln…C contact (per metal ion). In view of the latter

Table 3
Selected bond lengths (pm) and angles (°) of the complexes **3**–**5**

	3	**4**	**5**
Bond length (pm)			
Ln–C(1)	276.2(13)	281.7(15)	277.2(4)
Ln–C(2)	275.2(13)	278.2(14)	275.7(4)
Ln–C(3)	276.1(12)	276.0(14)	281.3(4)
Ln–C(8)	280.3(11)	285.4(16)	296.3(4)
Ln–C(9)	279.1(9)	280.5(13)	296.8(4)
Ln–Ct(51)	250.6	253.6	258.6
Ln–C(11)	276.3(10)	276(2)	284.2(4)
Ln–C(12)	275.6(14)	280(2)	282.2(4)
Ln–C(13)	279.1(12)	279(2)	286.1(4)
Ln–C(18)	278.9(8)	280.6(12)	297.7(4)
Ln–C(19)	282.1(12)	279.4(13)	301.5(4)
Ln–Ct(52)	251.3	252.0	264.1
Ln–C(21)	278.8(12)	278(2)	286.4(4)
Ln–C(22)	274.7(13)	277(2)	281.6(4)
Ln–C(23)	274.4(10)	278.0(13)	287.3(4)
Ln–C(28)	283.3(11)	284.4(15)	297.0(4)
Ln–C(29)	277.3(10)	281.0(11)	299.7(3)
Ln–Ct(53)	250.3	252.1	264.0
Bond angle (°)			
Ct(51)–Ln–Ct(52)	121.6	118.4	116.6
Ct(52)–Ln–Ct(53)	118.1	121.7	115.9
Ct(53)–Ln–Ct(51)	118.2	117.9	114.8

complex it should be pointed out that the radius of Sm(II) is only insignificantly longer than that of La(III) [12].

The polymeric nature of **5** is also reflected by its comparatively high melting point (e.g. **5**: 245–250°C; **4**: 168–172°C). Accounting thus explicitly for the intermolecular La…C bond, each molecule of **5** might also be considered as a kind of $[La(C_9H_7)_3 \cdot L]$ adduct. This view is supported by the *equatorial* orientation of two C_9H_7 ligands (vide supra) and a larger (than in **3** and **4**, see Table 2) distance of the La(III) ion from the plane spanned by the three C_5 ring centers of the C_9H_7 ligands. The conformation of this 'adduct' is somewhat reminiscent of the structural motif II displayed by one $[La(C_9H_7)_3 \cdot THF]$ modification [7]. Each $\{La(\mu\text{-}C_9H_7)\}$ fragment should, moreover, display planar chirality. However, in accordance with the achiral space group of **5**, these additional chirogenic centers adopt, like those based on the *equatorial* nature of two C_9H_7 ligands (vide supra), building blocks that turn out to be alternately opposite mirror images.

5. Solution studies

5.1. ^{1}H-NMR spectroscopy

At room temperature (r.t.), all base-free $[Ln(C_9H_7)_3]$ systems **1** and **3**–**5** display, as their earlier reported THF adducts [5,6], proton resonance patterns consistent with three virtually equivalent, and highly symmetrical (i.e. even with respect to mirror planes perpendicular to each individual C_9H_7 unit), indenyl ligands (Fig. 5). Obviously, these features indicate efficient and rapid (on the NMR time scale) equilibration of all three C_9H_7 ligands. Somewhat unexpectedly, in C_6D_6 solution, the resonances of the three H atoms of **5** in the positions 1, 2 and 3 even collapse into one symmetrical singlet. Fig. 6 shows that the (ideal) doublet/triplet combination of **5** undergoes various changes (both in appearance and chemical shift) between $+80$ and -50°C. Interestingly, the signals of the H atoms 1, 2 and 3 move towards the resonance range of aliphatic protons as the temperature is lowered.

In the spectra of **1**, **3** and **4**, almost all internuclear spin coupling is quenched owing to the paramagnetism of the central metal ions. The absence of any uncharged ligand L leads to some unexpected signal displacements. This feature is most pronounced for Ln = Pr, the signals of **4** being spread over a total range of 42.9 ppm, instead of only 12.5 ppm in the case of the THF-adduct [7]. In C_6D_6, the resonance of H-1/3 of **1**, **3** and **4** appears at lower field than that of H-2, whereas this sequence is reversed for the THF adducts of **3** and **4** [7] (as well as for neat **4** when dissolved in CD_2Cl_2).

In toluene-d_8, all four proton resonances of **4** display a very unusual temperature dependence (Fig. 7). None of the δ versus T^{-1} plots turns out to be a straight line, which behaviour would otherwise be expected for stable, paramagnetic molecules unaffected by any chemical equilibria [15]. Curves passing a maximum or minimum most likely result from the superposition of two individual, at least approximately straight lines of opposite slopes, owing to the interplay of (at least) two different, rapidly interconverting species. Usually, the concentrations of these equilibrating species vary strongly with temperature, too, which circumstance often helps magnifying the deviation from linearity of the resulting δ versus T^{-1} plot. In view of the tendency of **5** to form polymeric chains in the solid state (vide supra), it appears tempting to assume that this complex, and presumably also its Pr(III) homologue, **4**, undergo likewise oligo- and/or polymerization in non-polar solvents:

$$\underset{\text{high-temp. form}}{n[Ln(C_9H_7)_3]} \overset{\text{toluene}}{\underset{\text{(rapid)}}{\rightleftharpoons}} \underset{\text{low-temp. form(s)}}{[Ln(C_9H_7)_2(\mu\text{-}C_9H_7)]_n} \quad (2)$$

We have found earlier [15] that two of the three δ versus T^{-1} plots of base-free $[Pr(C_5H_4Me)_3]$ **6** dissolved in toluene-d_8 show likewise pronounced maxima. This unusual behaviour was interpreted as due to rapid equilibria involving both monomeric molecules and oligomeric aggregates, which hypothesis was subsequently supported by the finding that crystalline **6** contains tetrameric units [16]. Actually, the NMR spectrum of **6** passes between -10 and -50°C several

Table 4
Comparison of the parameters $\Delta = \langle Ln-C(8, 9)\rangle_{av} - \langle Ln-C(1, 2, 3)\rangle_{av}$ and ϕ (see text) of various structurally elucidated tris(indenyl)metal complexes

Complex	C_9H_7 (A)			C_9H_7 (B)			C_9H_7 (C)			Ref.
	Δ (pm)	ϕ (°)	Orientation	Δ (pm)	ϕ (°)	Orientation	Δ (pm)	ϕ (°)	Orientation	
$[(C_9H_7)_3La]$	18.5	6.2	*eq*	15.4	7.5	*mer*[b]	13.3	4.1	*eq*	This work
$[(C_9H_7)_3La\cdot THF]$	13.5	3.2	*mer*[b]	18.5	5.2	*eq*[c]	16.1	4.3	*mer*[c,d]	[7][e]
$[(C_9H_7)_3La\cdot THF]$	22.2/16.6	8.0/7.1	*eq*	18.5/8.9	6.1/3.9	*eq*/*mer*[c,d]	16.9/17.7	6.0/4.7	*eq*	[7][f]
$[(C_9H_7)_3La\cdot(R)-MTSO]$	17.3	5.9	*eq*	3.3	1.0	*eq*	13.8	2.0	*mer*[d]	[5]
$[(C_9H_7)_3Pr]$	4.3	3.8	*mer*[b,c]	1.7	0.7	*mer*	5.0	1.7	*mer*[b,c]	This work
$[(C_9H_7)_3Pr\cdot THF]$	24.3/19.7	8.2/6.8	*eq*	21.9/10.4	5.8/4.4	*eq*/*mer*[c,d]	18.1/21.4	5.5/4.5	*eq*/*mer*[c,d]	[7]
$[(C_9H_7)_3Pr\cdot(R)-MTSO]$[i]	18.6	5.9	*eq*	1.8	1.9	*eq*	13.1	4.1	*mer*[d]	
$[(C_9H_7)_3Nd]$	3.9	1.6	*mer*[b,c]	3.5	3.0	*mer*[b]	−0.2	3.8	*mer*[b,c]	This work
$[(C_9H_7)_3Nd\cdot THF]$	23.3/27.8	8.9/6.4	*eq*	21.2/11.0	8.9/4.6	*eq*/*mer*[c,d]	20.5/23.5	5.7/5.5	*eq*/*mer*[c,d]	[7][g]
$[(C_9H_7)_3Nd\cdot THF]$	23.3	7.3	*eq*	23.3	7.3	*eq*	23.3	7.3	*eq*	[7][h]
$[(C_9H_7)_3Nd\cdot DPSO]^I$	15.2/18.2	4.3/5.0	*eq*[c]	16.3/13.1	3.8/4.0	*mer*[b,c]	14.9/16.7	5.2/1.1	*eq*[c]	
$[(C_9H_7)_3Sm]$	7.0	—	*mer*	−5.0	—	—	8.0	—	—	[8]
$[(C_9H_7)_3Sm\cdot THF]$	25.6	7.1	*eq*	25.6	7.1	*eq*	25.6	7.1	*eq*	[7]
$[(C_9H_7)_3U]$	2.8	—	*mer*	4.4	—	*mer*	2.2	—	*mer*	[9]
$[(C_9H_7)_3UCl]$	12.8	—	*mer*[b]	9.7	—	*mer*[b]	18.8	—	*mer*[b]	[10]

Not reported: [a] *eq*, *equatorial*; *mer*, *meridional*. [b] *Cisoid* in regard to the axial ligand L. [c] Approximately. [d] *Transoid* in regard to the axial ligand L. [e] Sample **2** of [7]. [f] Sample **1** of [7]. [g] Sample **4** of [7]. [h] Sample **5** of [7]. [i] J.W. Guan, R.D. Fischer, unpublished results.

coalescence regimes, but consists at ca. −70°C again of several comparatively sharp signals one of which is in fact strongly high-field shifted [15]. At least one of the resonances of **6** would be expected to display a strongly inverse temperature characteristic.

The resonances of **4** undergo considerable broadening around −70°C, too, although the final spectrum of the low-temperature form could still not be observed above the melting point of the solvent. Toluene-d_8 solution of **4**/**5**-mixtures (ca. 5:4) give again rise to the four individual ^1H resonances of either complex, ruling thus out any rapid intermolecular C_9H_7 ligand exchange. More surprisingly, the actual positions of the resonances of neither complex are notably affected by the quite different magnetic properties of the accompanying complex. Hence, the presence of, inter alia, short-lived bimetallic $\{(C_9H_7)_3La(\mu\text{-}C_9H_7)Pr(C_9H_7)_2\}$ fragments is not clearly reflected by this particular NMR experiment.

In accordance with its better capability to cleave oligomeric species, the more polar solvent CD_2Cl_2 was shown to generate in the case of **6** three strictly linear δ versus T^{-1} plots [15], while, somewhat unexpectedly, two still non-linear curves (albeit devoid of any extrema) result for the resonances of **4** (Fig. 8). One of these curves even indicates an inverse temperature dependence, in that $|\delta|$ decreases when the temperature is lowered. Quite unexpectedly, also the resonances of the solvent (toluene-d_8) of **4** display below −20°C a significant temperature dependence (referred here to TMS as internal standard). Thus the main signal of the arene protons moves from ca. 7.20 ppm at −20°C continuously to ca. 12.5 ppm at −80°C, and the methyl proton resonance from 2.26 to 7.52 ppm. This finding suggests non-negligible chemical interaction of solvent molecules with the paramagnetic Pr(III) centers of **4**, as a potential alternative of its self-association. The actual magnitude of the low-field displacement of the solvent resonances is quite remarkable in view of (a) the high excess of the solvent molecules and (b) the very low amount of residual protons in the almost exhaustively deuterated toluene molecules.

5.2. Electronic spectra of *4*

Fig. 9 shows for comparison the optical absorption spectra between 430 and 650 nm of **4** and its THF adduct in benzene solution. Both spectra are dominated by the widely extended low-energy wings of a very strong charge-transfer band reaching its maximum long below 350 nm. The low-energy wing of **4** is even more intense than that of the adduct, as not only the narrow f–f crystal field bands between 450 and 520 nm, but also those between 590 and 630 nm (of **4**) are buried under its low-energy CT wing. Evidently, the absence of the Lewis base (THF) causes a significant bathochromic shift of the CT band, which feature is also responsible for the different colours of **4** and its THF-adduct.

Andersen et. al. have reported that the base-free tris(cyclopentadienyl)cerium(III) complexes [Ce(C_5H_5-

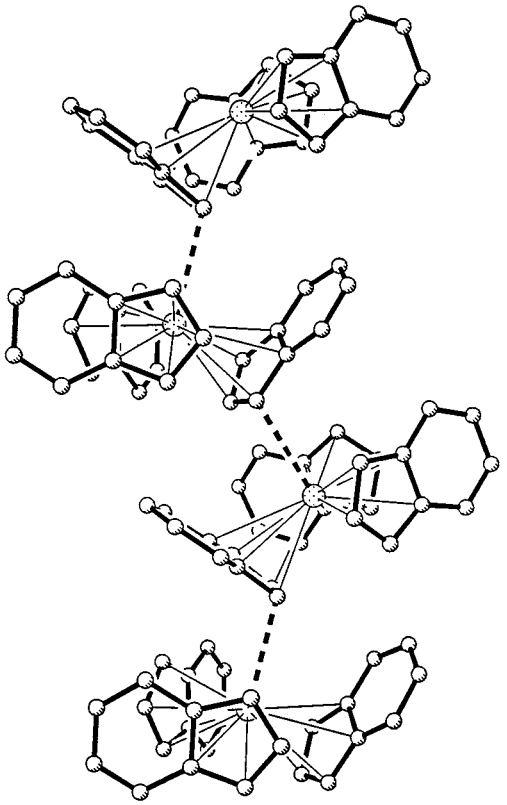

Fig. 4. Tetramolecular fragment of an infinite zigzag chain of polymeric **5**.

R)$_3$] are blue, while the corresponding base adducts, including even the tetranuclear 'adduct' [Ce(C_5H_4Me)$_2$(μ-η^1:η^5-C_5H_4Me)]$_4$ are yellow [13]. However, NIR–vis spectroscopic results are still missing. Both Ce(III) and, to a lesser extent, Pr(III) are susceptible to oxidation so that in both cases a corresponding metal-to-ligand CT is most probable.

Although below 630 nm the f–f CF absorption bands of **4** are strongly obscured (see Fig. 9), these transitions may nevertheless be detected indirectly. Actually, it has turned out that the magneto-circular dichroism (MCD) of the genuine f–f bands is more pronounced than that of the (side wing of the) broad CT band [7]. In Fig. 10, the MCD of **4** dissolved in C_6H_6 and CH_2Cl_2 is compared with the earlier reported MCD of the THF adduct. Strictly speaking, all three spectra are different, which finding agrees in principle with the ^{1}H-NMR spectroscopic features reported above.

6. Experimental

All experimental manipulations and measurements were carried out as described previously [7]. To prepare the strictly base-free title compounds [Ln(C_9H_7)$_3$] with Ln = Sm **1**, Nd **3**, Pr **4** and La **5**, the corresponding THF-adducts [7] were subjected at temperatures between 120 and 150°C to a vacuum of at least 1×10^{-3} mbar. After 5–8 h, the majority of the product usually remained as a fine powder on the bottom of the Schlenk tube, while smaller portions of the product were sublimed and redeposited close to that powder. Both portions were redissolved in hot toluene. After filtration, slow cooling and transfer of the filtrate into the refrigerator (ca. 0°C), ideally-shaped single crystals, suitable for crystallographic X-ray studies, became available after a few days.

6.1. Complex *1*

[Sm(C_9H_7)$_3$] **1** (m.p. 161–165°C) elemental analysis $C_{27}H_{21}Sm$ calc. 65.45, H 4.23; found: C 64.62, H 4.34%. MS (*m*/*e*): 494, 382, 267, 152 and 115 for {Sm(C_9H_7)$_n$}$^+$ with $n = 3$, 2, 1, 0 and $C_9H_7^+$, respectively. Selected IR absorption (KBr pellet, cm^{-1}): 3064(s), 1700(br, m), 1605(w), 1554(w), 1457(s), 1393(s), 1360(m), 1329(s), 1239(w), 1216(m), 1168(s), 1121(s), 1068(br, s), 1018(w), 969(s), 942(w), 915(w), 885(w), 862(w), 767(vs), 745(w), 718(w), 696(m),

Table 5
Survey of relevant metal-to-carbon distances (pm) in some related oligo- or polymeric systems

Poly- or oligomeric species	Shortest intermolecular Ln…C distance (pm)		Ref.
[La(η^5-C_5H_5)$_2$(μ-η^2:η^5-C_5H_5)]$^a_\infty$	303.2(6)	303.4(6)	[17]
[La(η^5-C_5H_5)$_2$(μ-η^1:η^5-C_5H_5)]$^b_\infty$	297.2(7)	299.9(8)	[18]
[La(η^5-C_5H_4Me)$_2$(μ-η^1:η^5-C_5H_4Me)]$^b_4$	297.2(5)	306.4(6)	[19]
	297.2	306.1	[16]
[La(η^5-C_9H_7)$_2$(μ-η^1:η^5-C_5H_7)]$_\infty$ (**5**)	309.7(4)	329.4	This work
[Ce(η^5-C_5H_4Me)$_2$(μ-η^1:η^5-C_5H_4Me)]$^b_4$	297(1)	309(1)	[13]
[Sm^{II}(η^5-C_5H_5)$_2$(μ-η^2:η^5-C_5H_5)Sm^{III}(η^5-C_5Me_5)$_2$]	298.6(8)	318.0(9)	[20]

[a] One singular μ-C_5H_5 (or C_9H_7-) ligand present. [b] Two nonequivalent μ-C_5H_5 (or C_5H_4Me-) ligands exist.

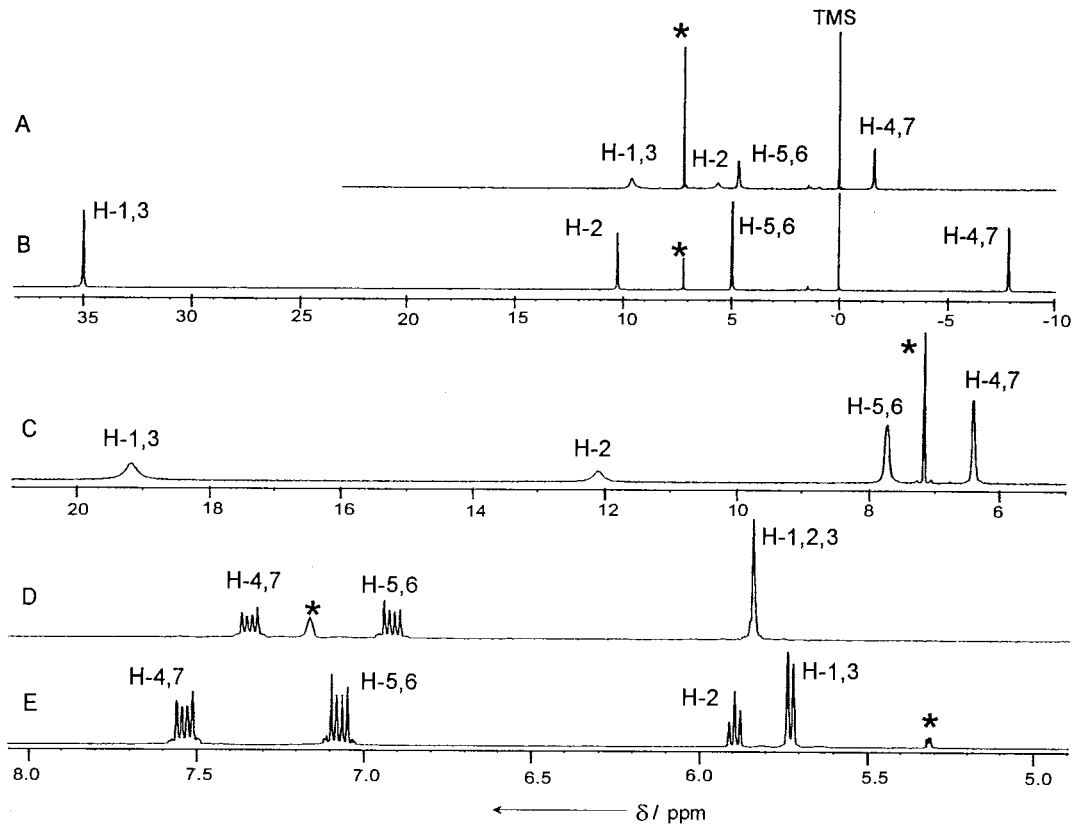

Fig. 5. Room temperature ^{1}H-NMR spectra (in C_6D_6) of **3** (A), **4** (B), **1** (C) and **5** (D). E depicts the spectrum of **5** in CD_2Cl_2 solution.

646(w), 569(w), 551(w), 534(w). ^{1}H-NMR (C_6D_6/TMS): 19.02(s, 6H), H-1,3; 12.06(s, 3H), H-2; 7.17(s, 6H), H-5,6; 6.39(s, 6H), H-4,7. In CD_2Cl_2/TMS: 15.06(s, 6H), H-1,3; 12.70(s, 3H), H-2; 7.94(s, 6H), H-5,6; 7.63(s, 6H), H-4,7.

6.2. Complex *3*

[Nd[C_9H_7)$_3$] **3** (m.p. 125–130°C) elemental analysis $C_{27}H_{21}Nd$ calc.: C 66.25, H 4.29; found C 65.78; H 4.41%. MS (*m*/*e*): 489, 372, 257, 142 and 115 for $\{Nd(C_9H_7)_n\}^+$ with $n = 3$, 2, 1, 0 and $C_9H_7^+$, respectively. Selected IR absorption (KBr pellet, cm^{-1}): 3068(w), 2953(m), 1685(m), 1618(w), 1604(w), 1458(s), 1392(s), 1364(m), 1330(w), 1244(w), 1167(w), 1122(w), 1068(w), 1018(w), 946(m), 914(m), 861(m), 766(vs), 718(s), 693(s), 551(m, br). ^{1}H-NMR (C_6D_6/TMS): 9.47(s, 6H), H-1,3; 5.68(s, 3H), H-2; 4.63(s, 6H), H-5,6; −1.70(s, 6H), H-4,7.

6.3. Complex *4*

[Pr[C_9H_7)$_3$] **4** (m.p. 168–172°C) elemental analysis $C_{27}H_{21}Pr$ calc. C 66.69, H 4.32; found C 65.19; H 4.38%. MS(*m*/*e*): 486, 371, 256, 141 and 115 for $\{Pr(C_9H_7)_n\}^+$ with $n = 3$, 2, 1, 0 and $C_9H_7^+$, respectively. Selected IR absorption (KBr pellet, cm^{-1}): 3065(m), 1675(br, m), 1628(m), 1553(m), 1457(s), 1393(s), 1360(m), 1329(s), 1246(m), 1216(w), 1167(s), 1120(s), 1068(br, s),1018(w), 970(m), 942(s), 915(w), 884(w), 862(m), 766(vs), 718(m), 694(w), 644(w), 551(m, br). ^{1}H-NMR (C_6D_6/TMS): 34.96(s, 6H), H-1,3; 10.24(s, 3H), H-2; 4.93(q, 6H), $J \approx 3.0$, H-5,6; −7.94(dd, 6H), $J = 2.72$, 3.60, H-4,7. In CD_2Cl_2/TMS: 15.41(s, 6H), H-1,3; 19.39(s, 3H), H-2; 7.27(s, 6H), H-5,6; 2.68(s, 6H), H-4,7.

6.4. Complex *5*

[La[C_9H_7)$_3$] **5** (m.p. 245–250°C) elemental analysis $C_{27}H_{21}La$ calc. C 66.97, H 4.34; found C 66.11; H 4.41%. MS (*m*/*e*): 484, 369, 254 and 115 for $\{La(C_9H_7)_n\}^+$ $n = 3$, 2, 1 and $C_9H_7^+$, respectively. IR absorption (KBr pellet, cm^{-1}): 3066(m), 2886(w), 1676(br, s), 1605(s), 1554(m), 1457(s), 1393(m), 1310(w), 1329(s), 1289(w), 1217(w), 1205(w), 1168(s), 1121(s), 1069(s, br), 1018(w), 968(s), 942(m), 915(w), 767(vs), 736(w), 718(m), 694(m), 644(m), 551(m, br).

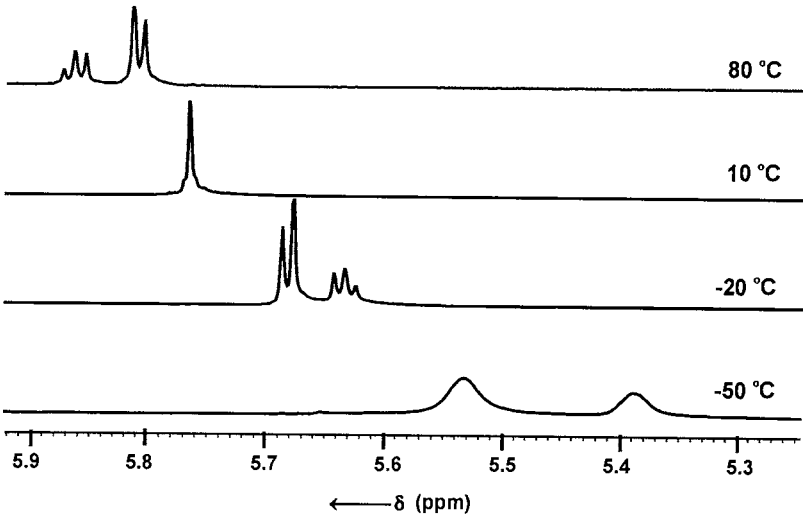

Fig. 6. Variable-temperature resonances of the indenyl protons 1, 2 and 3 of **5** (solvent: toluene-d_8).

^{1}H-NMR (C_6D_6/TMS): 5.81(s, 9H), H-1,2,3; 6.91(q, 6H), J ≈ 3.0, H-5,6; 7.34(q, 6H), J ≈ 3.0, H-4,7. In CD_2Cl_2/TMS: 5.72(d, 6H), $J = 3.22$, H-1,3; 5.89(t, 3H), $J = 3.36$, H-2; 7.07(q, 6H), J ≈ 3.0, H-5,6; 7.53(q, 6H), J ≈ 3.0, H-4,7.

Optical absorption spectra were recorded on a Cary 5-E spectrometer, and the corresponding MCD spectra on a Jasco J-500 C dichrograph equipped with a DP-500 N data processor and an electromagnet of a maximum field strength of 13.5 kG.

Promising single crystals were embedded in silicon oil for protection and selected thereafter under the microscope. The crystal of **5** was directly mounted onto the end of a glass fiber and measured at a temperature of −120°C on the Y290 (Hilger and Watts) diffractometer. For better comparison with **5**, another crystal of **3** was, likewise, studied at −120°C. The crystal data did not differ from those obtained at r.t., although the data set in total was of a slightly lower quality. Crystals of **3** and **4** were coated by silicon oil and placed rapidly in carefully conditioned, thin-walled Lindemann capillaries. The sealed capillaries were positioned on the Syntex $P2_1$ diffractometer and the crystals studied at r.t. The unit cell parameters and the crystal orientation matrix were determined by standard techniques making use of X-ray photographs and at most 25 reflections to arrive at least-squares refinements of the cell parameters, in analogy to the procedure described by Churchill et al. [21].

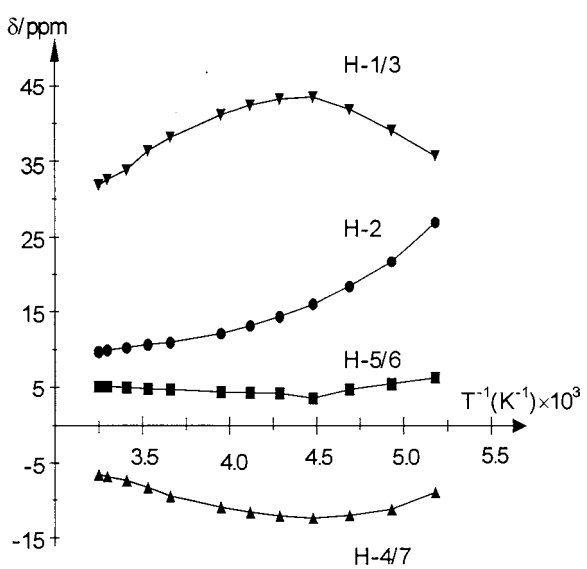

Fig. 7. δ versus T^{-1} plots of the proton resonances of **4** (solvent: toluene-d_8).

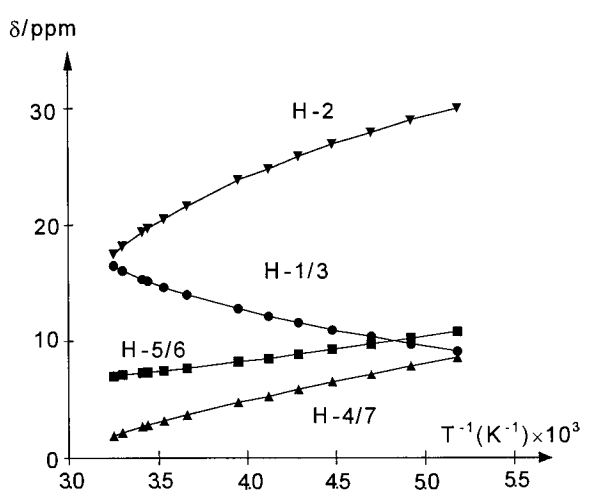

Fig. 8. δ versus T^{-1} plots of the proton resonances of **4** (solvent: CD_2Cl_2).

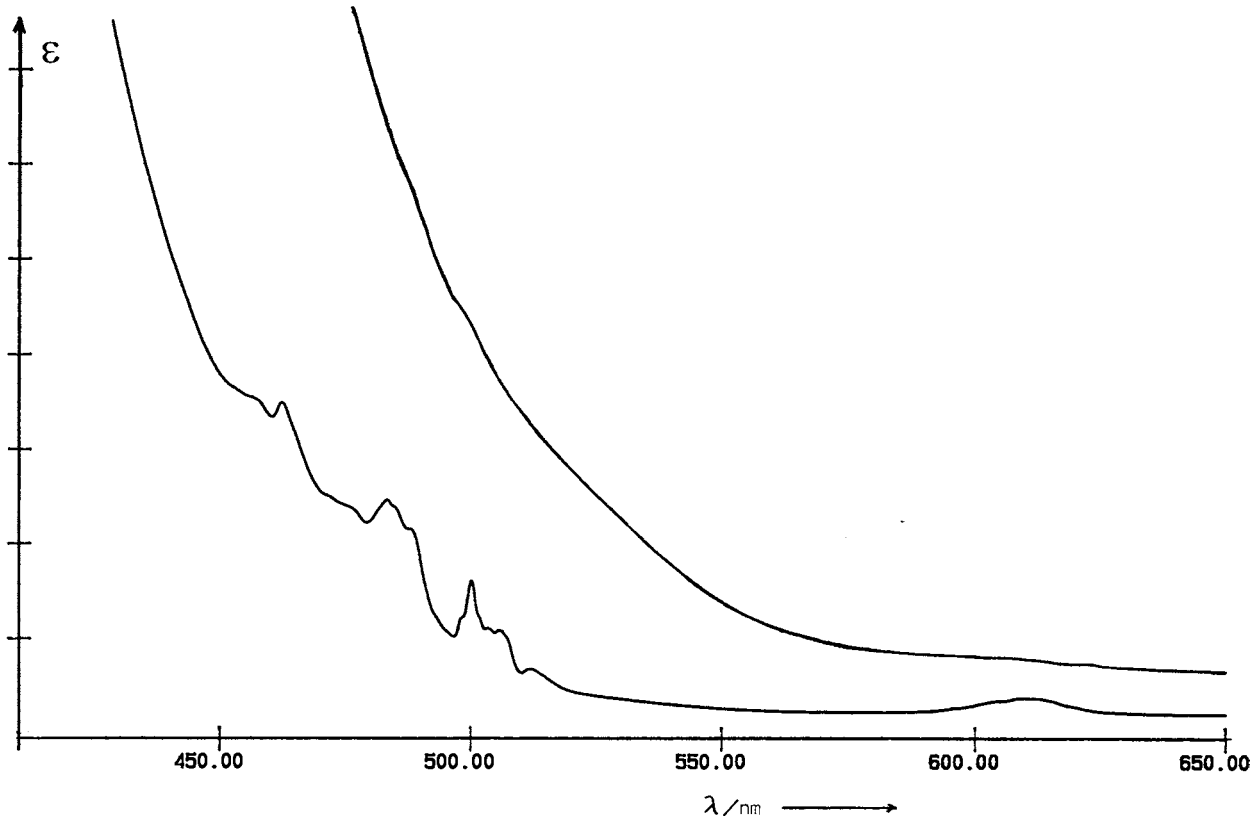

Fig. 9. Optical absorption spectra of **4** (above) and **4**·THF (below).

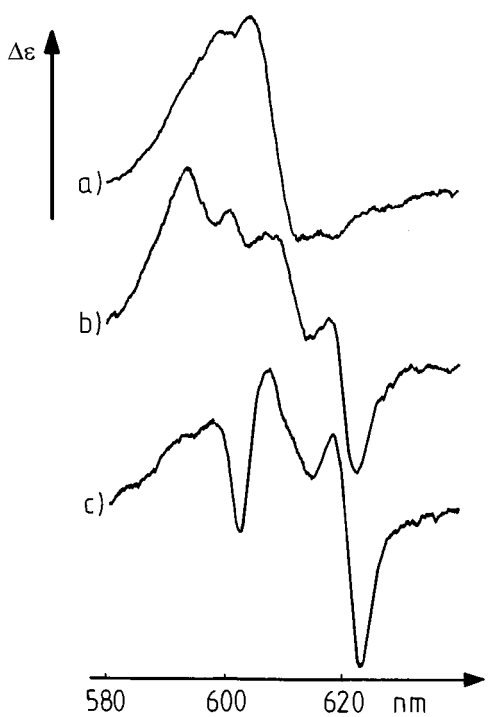

Fig. 10. MCD spectra of f–f excitations (to states of the $^1D_2$ manifold) of **4**·THF (a) and base-free **4** in CD_2Cl_2 (b) and C_6H_6 (c).

All crystallographic calculations were carried out by means of the SHELX-93 and SHELXTL-PLUS program set [22]. Heavy atoms were found from Patterson maps and there after the other non-H atoms were detected by different Fourier synthesis techniques. Furthermore, the structure models were refined by full-matrix least-squares techniques. Hydrogen atoms were included using a riding model with $d(C–H) = 97$ pm. Finally, all non-H atoms were refined anisotropically to convergence. Further details of the crystal structure investigation may be obtained from the Fachinforma- tionszentrum Karlsruhe, D-76344 Eggenstein-Leopoldshafen, Germany, on quoting the depository numbers CSD-408276, CSD-408277 and CSD-408278 for **3**, **4** and **5**, respectively.

Acknowledgements

The authors express their deep gratitude to the Friedrich-Ebert-Stiftung (Bonn) for the donation of a fellowship to J. Guan, and to Professor U. Behrens (Hamburg) for his kind supervision of the crystal structure analyses.

References

[1] Y. Su, Z. Jin, W. Chen, J. Chin. Rare Earth Soc. 8 (1990) 106.
[2] J. Xia, Zh. Jin, G. Lin, W. Chen, J. Organomet. Chem. 408 (1991) 173.
[3] Z. Ye, S. Wang, D. Kong, X. Huang, J. Organomet. Chem. 491 (1995) 57.
[4] S. Wang, D. Kong, Z. Ye, X. Huang, J. Organomet. Chem. 496 (1995) 37.
[5] J.-W. Guan, R.D. Fischer, J. Organomet. Chem. 532 (1997) 147.
[6] Q. Shen, M. Qi, S. Song, L. Zhang, Y. Lin, J. Organomet. Chem. 549 (1997) 95.
[7] J.-W. Guan, Q. Shen, R.D. Fischer, J. Organomet. Chem. 549 (1997) 203. In all numbers given in Table 4 of this paper, the comma has to be shifted one position to the left. Moreover, in Table 7, the references 27 and 28 should be exchanged (fifth column).
[8] J.L. Atwood, J.H. Burns, P.G. Laubereau, J. Am. Chem. Soc. 95 (1973) 1830.
[9] J. Meunier-Piret, J.P. Declercq, G. Germain, M. Van Meerssche, Bull. Soc. Chim. Belg. 89 (1980) 121.
[10] J.M. Burns, P.G. Laubereau, Inorg. Chem. 10 (1971) 2789.
[11] M.R. Spirlet, J. Rebizant, J. Goffart, Acta Crystallogr. C 34 (1987) 354.
[12] R.D. Shannon, Acta Crystallogr. A 32 (1976) 751.
[13] S.D. Stults, R.A. Andersen, A. Zalkin, Organometallics 9 (1990) 115.
[14] M. Tsutsui, H.J. Gysling, J. Am. Chem. Soc. 91 (1969) 3175.
[15] W. Jahn, K. Yünlü, W. Oroschin, H.-D. Amberger, R.D. Fischer, Inorg. Chim. Acta 95 (1984) 85 and further references cited therein.
[16] H. Breitbach, Doctoral Dissertation, Universität Hamburg, Germany, 1987, p. 6.
[17] S.H. Eggers, J. Kopf, R.D. Fischer, Organometallics 5 (1986) 383.
[18] J. Rebizant, C. Apostolidis, M.R. Spirlet, B. Kanellakopulos, Acta Crystallogr. C 44 (1988) 614.
[19] Z. Xie, F.E. Hahn, C. Qian, J. Orgnaomet. Chem. 414 (1991) 12.
[20] W.J. Evans, T.A. Ulibarri, J. Am. Chem. Soc. 109 (1987) 4292.
[21] M.R. Churchill, R.A. Lashewycz, F.J. Rotella, Inorg. Chem. 16 (1977) 265.
[22] (a) G.M. Sheldrick, SHELX-86, Acta Crystallogr. A 46 (1990) 467. (b) G.M. Sheldrick, SHELX-93, Program for the Refinement of Crystal Structures, Universität Göttingen, Germany, 1993. (c) G.M. Sheldrick, SHELX-PLUS, Release 4.21/v, Siemens Analytical X-ray Instruments, Madison, WI.